Quantum-Dot Cellular Automata at a Molecular Scale

MARYA LIEBERMAN,[a] SUDHA CHELLAMMA,[a] BINDHU VARUGHESE,[a] YULIANG WANG,[a] CRAIG LENT,[b] GARY H. BERNSTEIN,[b] GREGORY SNIDER,[b] AND FRANK C. PEIRIS[b,c]

[a]*Department of Chemistry and Biochemistry, University of Notre Dame, Notre Dame, IN 46556, USA*

[b]*Department of Electrical Engineering, University of Notre Dame, Notre Dame, IN 46556, USA*

ABSTRACT: Quantum-dot cellular automata (QCA) is a scheme for molecular electronics in which information is transmitted and processed through electrostatic interactions between charges in an array of quantum dots. QCA wires, majority gates, clocked cell operation, and (recently) true power gain between QCA cells has been demonstrated in a metal-dot prototype system at cryogenic temperatures. Molecular QCA offers very high device densities, low power dissipation, and ways to directly integrate sensors with QCA logic and memory elements. A group of faculty at Notre Dame has been working to implement QCA at the size scale of molecules, where room-temperature operation is theoretically predicted. This paper reviews QCA theory and the experimental measurements in metal-dot QCA systems, and describes progress toward making QCA molecules and working out surface attachment chemistry compatible with QCA operation.

KEYWORDS: cellular automata; mixed-valence compounds; molecular electronics; quantum dots; single-electron devices

INTRODUCTION

Molecular Electronics and Quantum-Dot Cellular Automata

Most approaches to molecular electronics have sought to reproduce conventional electronic elements, such as transistors, wires, or diodes.[1] To this date, no one has demonstrated a molecular electronic device that functions in concert with others. As in conventional electronics, connecting the device components is a major problem. The output current from a single conductive molecule is in the nanoampere region, and current conduction in a molecule dissipates large amounts of energy. Yet to change the electronic state of a molecule—to switch a molecular transistor on or off

Address for correspondence: Marya Lieberman, Department of Chemistry and Biochemistry, 252 NSH, University of Notre Dame, Notre Dame, IN 46556. Voice: 219-631-4665; fax 219-631-6652.
mlieberm@nd.edu
[c]Current address: Department of Physics, Kenyon College, Gambier, OH 43022.

Ann. N.Y. Acad. Sci. 960: 225–239 (2002).

— a signal of the order of volts must be applied.[2] Using one molecule as a transistor to switch another is therefore difficult, and the difficulty multiplies with the number of molecular components that must be connected.

A group of electrical engineers and chemists at Notre Dame is developing and implementing quantum-dot cellular automata (QCA) as a new architecture for molecular electronics. QCA is a radical departure from conventional microelectronics, and is already influencing other workers in the field of molecular electronics.[3–5]

The QCA approach exploits the molecule as a *structured charge container.* One molecule's state is communicated to its neighbors through Coulomb forces. Remarkably, this interaction is sufficient to enable general-purpose computing.

There is a key place for current-carrying molecules in the QCA paradigm — as inputs and electrometers. Electrometers are necessary to sense the state of output cells and communicate this information to the macroscopic world. We are developing a variety of detectors to sense the state of output cells, but in the long term, molecular wires bridging macroscopic electrodes, such as those made by Tour and Reed,[6] would be a natural solution to integrated I/O. These detectors could then be coupled to CMOS amplifiers to bring signal levels up.

THEORY AND EXPERIMENTS

QCA Theory

A schematic diagram of an idealized four-dot QCA cell is shown in FIGURE 1a. The cell consists of four quantum dots positioned at the corners of a square. The cell contains two extra mobile electrons, which can tunnel between neighboring sites of the cell. Tunneling out of the cell is assumed to be completely suppressed. The compensating positive charge is fixed and immobile. The four-dot cell can also be viewed as two double-dot cells arranged side by side, and indeed this is the way that QCA cells have been experimentally implemented at the micron scale.

If the barriers between cells are sufficiently high, the electrons will be well localized on individual dots. The Coulomb repulsion between the electrons will tend to make them occupy antipodal sites in the square as shown in FIGURE 1b. For an isolated cell there are two energetically equivalent arrangements of the extra electrons which we denote as a cell polarization $P = +1$ and $P = -1$. The term "cell polarization" refers only to this arrangement of charge and does not imply a dipole moment for the cell. The cell polarization is used to encode binary information, thus, $P = +1$ represents a binary **1** and $P = -1$ represents a binary **0.**

The two polarization states of the cell will not be energetically equivalent if other cells are nearby. Consider two cells close to one another as shown in the inset of FIGURE 2. The figure inset illustrates the case when cell 2 has a polarization of +1. It is

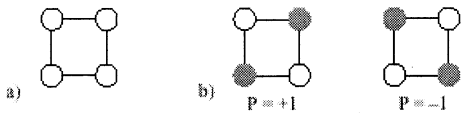

FIGURE 1. Schematic four-dot QCA cell.

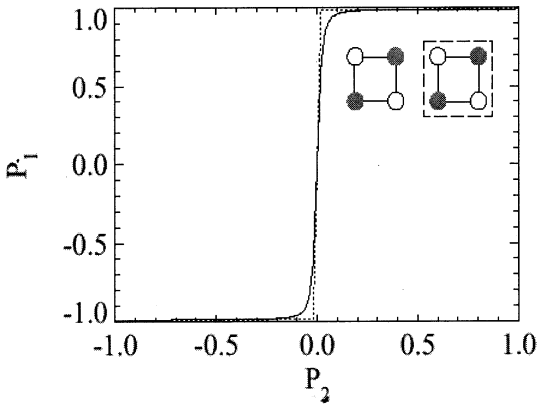

FIGURE 2. Nonlinear interaction between QCA cells.

clear that in that case the ground-state configuration of cell 1 is also a +1 polarization. Similarly if cell 2 is in the $P = -1$ state, the ground state of cell 1 will match it. The figure shows the nonlinear response of the cell–cell interaction to which plays the role of voltage gain in conventional devices — restoring signal levels at each stage.

QCA devices

The architecture required for both simple and complex QCA devices is basically established.[7] A QCA wire is shown in FIGURE 3a. The left-most cell is fixed with a polarization representing the input. The ground-state configuration of the remaining free cells is then one with each cell polarized in the same way as the input cell. Thus, the input signal is propagated along the wire without electrical current.

Cells that are positioned diagonally from each other tend to antialign. This feature is employed to construct an inverter as shown in FIGURE 3b. The antialignment can also be seen by examination to be a simple consequence of the mutual repulsion between electrons and the geometry of the cells. Although two diagonal cells function as an inverter, this more symmetric design ensures exact symmetry between the inversion of a 1 and a 0. Fan-out of a signal is illustrated in FIGURE 3c.

FIGURE 3d shows the fundamental QCA logical device, a three-input majority gate, from which more complex circuits can be built. The central cell, labeled the device cell, has three fixed inputs, labeled A, B, and C. The device cell has its lowest energy state if it assumes the polarization of the majority of the three input cells. The output can be connected to other wires from the output cell. The schematic symbol used to represent such a gate is also shown in FIGURE 3d. It is possible to "reduce" a majority logic gate by fixing one of its three inputs in the 1 or 0 state. If the fixed input is in the 1 state, the OR function is performed on the other two inputs. If it is fixed in the 0 state, the AND function is performed on the other two inputs. In this way, a reduced majority logic gate can also serve as a programmable AND/OR gate. QCA devices provide logical completeness for general-purpose computing.

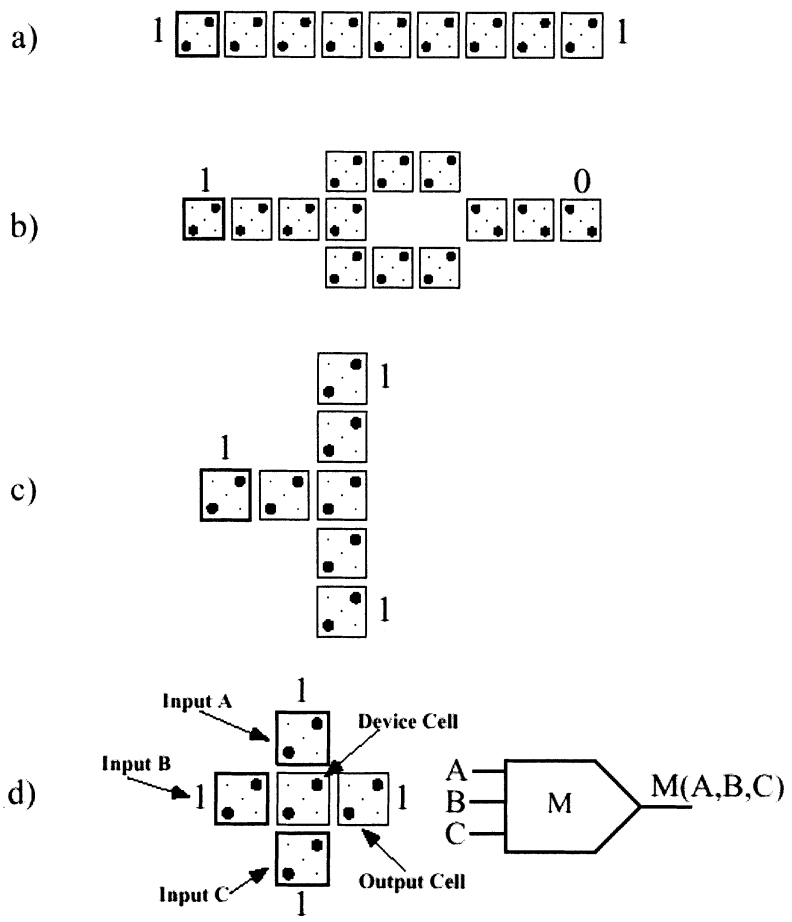

FIGURE 3. QCA devices. (**a**) Wire; (**b**) inverter; (**c**) fan-out; (**d**) majority gate.

Experimental Demonstration of QCA at Micron Scale

QCA has now been demonstrated in micron-sized metal cells, wires, and majority gates at very low temperatures. Snider *et al.* have fabricated and tested a variety of QCA devices based on metal dots on an oxidized silicon substrate. An early demonstration consisted of a four-dot cell built from two double-dot cells.[8] This experiment confirmed that the switching of a single electron in a double-dot cell can control the position of a single electron in another double-dot cell.[9] These metal dot tunnel-junction cells operate at 80 mK, but even within the tunnel-junction paradigm it is clear that as sizes of dots and junctions shrink, operating temperatures increase.[10] Molecular scales (~2 nm) are predicted to yield room-temperature QCA operation.[11]

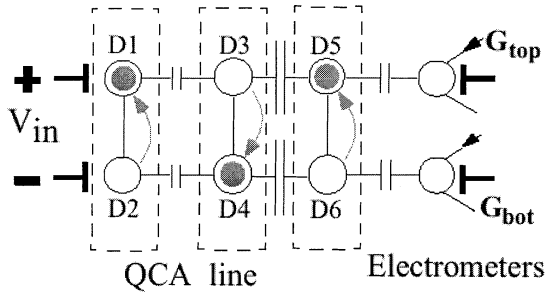

FIGURE 4. Schematic diagram of metal-dot QCA wire; experimental data shown in FIGURE 5.

One criticism of the QCA architecture[12] asserts that even a slight variation of the coupling capacitances along a line will cause errors due to metastable states. The claim is that when an input to a line changes, the polarization change will propagate along a line, but stop at a defect (weaker coupling), since the cell further along the line (with stronger coupling) will keep the weakly coupled cell from changing its polarization. A schematic diagram of a line of three two-dot metallic cells (a QCA "wire") using our metal tunnel junction technology is shown in FIGURE 4. By placing an *intentional defect* in the line, we tested the error tolerance of a QCA "wire."[13] The coupling capacitances between the first and second half-cells were one-third the value of the capacitances coupling the second and third cells.

Our experimental results show that this is not a problem, as illustrated in FIGURE 5. Plotted in the top panel, as a function of the differential input voltage applied to the first cell, is the measured potential of the top dot in the last cell of the line, D5, along with the theoretical potential at a temperature of 75 mK. The polarization of the line switches at an input of 0 V, indicated by the change in the potential. The excellent agreement between experiment and theory allows us to calculate the electron occupancy of each of the cells. The lower three panels show the calculated charge on the dots of each cell. The first cell undergoes a complete polarization charge change of 1 *e*. While there is a decrease in the polarization change at the weakly coupled second cell, it and the subsequent cell do switch. This decrease in the polarization is due mainly to temperature smearing effects. Since the energy scales in molecules are much larger, we anticipate switching of a line of molecular cells to be feasible at room temperature. This result also indicates that there will be considerable tolerance of cell placement errors and other defects which cause reduced coupling between cells.

We have recently demonstrated a *majority gate* using metal dots with three differential input voltages, A, B, and C. The measured output waveform is shown below in FIGURE 6. The applied gate voltages are set to the experimental potential swing obtained by switching an electron within a double-dot, approximately 110 μV. A binary sequence of the possible inputs is applied to the majority gate, and the resulting electrometer measurement of the output is plotted in FIGURE 6 along with the theoretical output at 75 mK. The gate exhibits the proper majority function, and shows good separation between "on" and "off" output voltage.

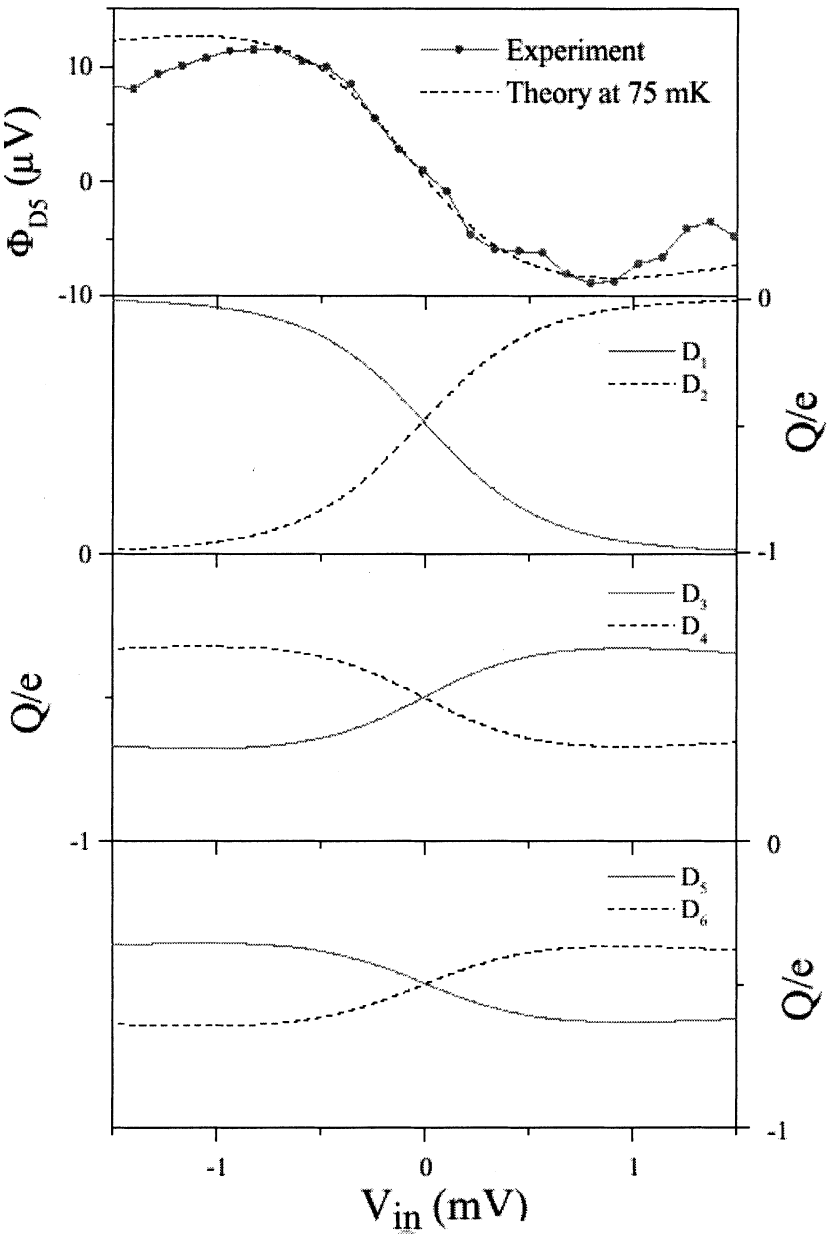

FIGURE 5. Experimental output at 75 mK (*top panel, dotted line*) and simulated output (*top panel, dashed line*) from the metal-dot QCA wire shown in FIGURE 4. The coupling capacitance between the first and second two-dot cells is about 0.33 of the coupling capacitance between the second and third two-dot cells. *Bottom three panels* show calculated charges on the dots of each individual cell.

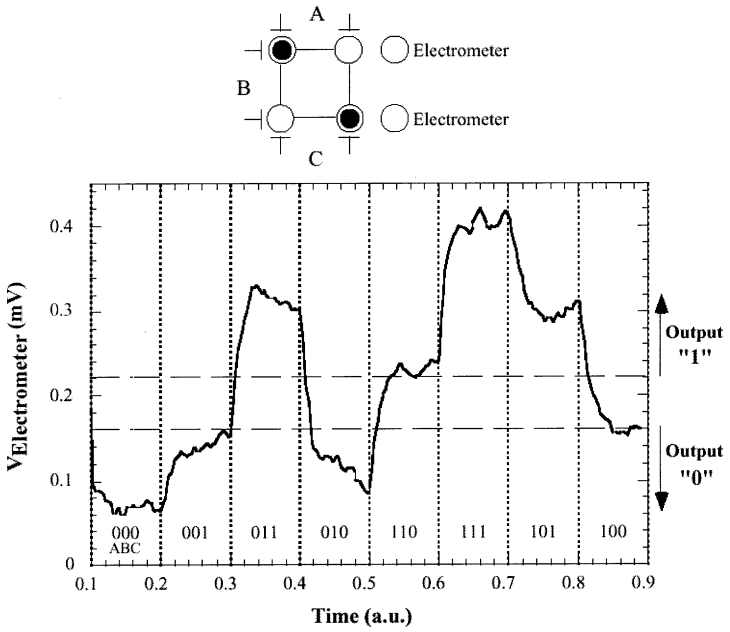

FIGURE 6. Schematic diagram and experimental output for metal-dot QCA majority gate as a function of all possible combinations of the three output signals.

The majority gate can be used for triple-modular redundancy error correction. Each medium-level function implemented by a QCA array can be evaluated in three redundant arrays, with the results fed into a voter cell. A simple version of this approach results in an overall error probability which is the square of the error probability of the individual arrays.

These "prototype" QCA devices operate only below 100 mK because the metal dots are so large that they must be operated in the Coulomb blockade temperature regime. We are now in the process of implementing QCA devices at the very smallest size scale possible, the scale of individual molecules. At this size scale, electronic coupling and electrostatic interactions create couplings and energy differences on the electron volt scale. Since the thermal energy available at room temperature is only about 0.025 eV, molecular-sized QCA cells are predicted to operate at room temperature. The systems used to provide input and output to arrays of QCA cells must function at the operational temperature of the QCA cells, in addition to meeting extremely high standards for sensitivity and stability. We have been able to meet these requirements in the case of micron-sized QCA cells, wires, and majority gates; in the process we have demonstrated the validity of the QCA paradigm.

Molecular QCA Cells

Room-temperature operation requires QCA cells in the 1–5-nm size range. Metallic and semiconducting quantum dots in this size range are synthetically available

now, but their sizes are heterogeneous and there are no good ways to stick them together on surfaces into two-dot or four-dot QCA cells with the requisite tunneling junctions. Fabrication of nanometer-scale QCA cells is clearly a problem for chemists.

The requirements for molecules analogous to the micron-scale two-dot cells are:

(1) Two electrochemically reversible and chemically stable redox centers held at a fixed distance of 1–5 nm.
(2) Strong coupling between the redox centers (to allow tunneling of the charge).
(3) A stable mixed-valence state with a comproportionation constant (K_{com})of at least 10^5.

Many mixed-valence metal compounds (such as the Creutz-Taube ion) easily meet these requirements and are worth a look as QCA cells. Initially, this is what we tried. We soon discovered that, although the Creutz-Taube ion has suitable electrochemical properties, it (and related highly charged compounds) brings along many counterions when it binds to surfaces.

Molecular QCA cells must be attached to surfaces in ordered arrays. We are using electron-beam lithography to burn narrow "tracks" along surfaces. We have partially characterized the chemical nature of the tracks and are studying the binding of QCA molecules to surfaces that mimic the track chemistry.

Surface Binding Properties of $[(NH_3)_5RupzRu(NH_3)_5]^{4+,\,5+}$

The Creutz-Taube ion $[(NH_3)_5RupzRu(NH_3)_5]$ was synthesized in its +4 and +5 (mixed-valence) oxidation states using literature procedures.[14] Despite its desirable properties (two reversible one-electron oxidations, a K_{com} of 3×10^5, an intense charge-transfer band, and stability to air and water), its surface attachment properties proved unsuitable for QCA arrays. Model hydrophilic (Si/SiO_2, contact angle <30°)

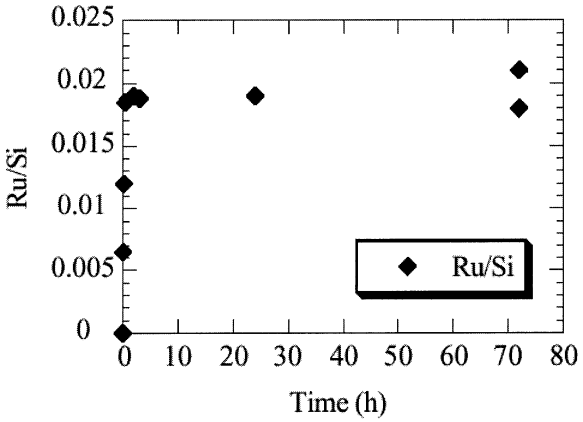

FIGURE 7. Creutz-Taube ion binding to silicon oxide; ruthenium:silicon XPS signal vs. soaking time.

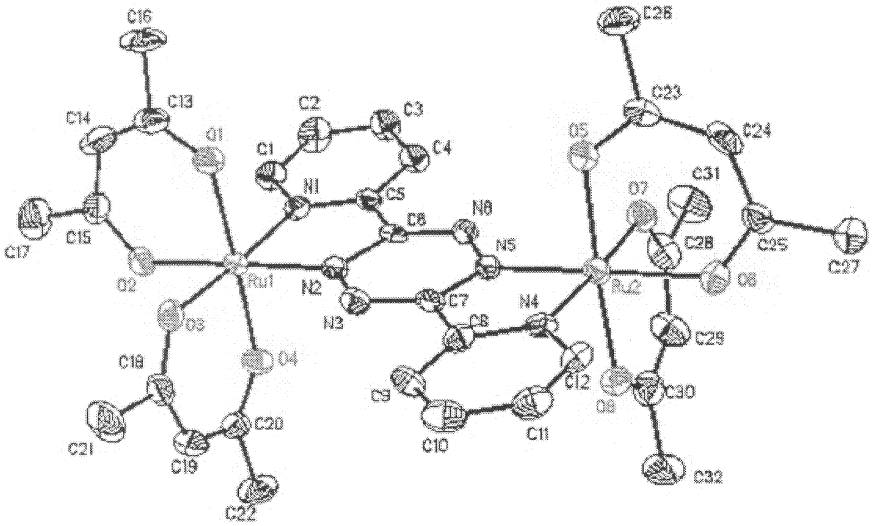

FIGURE 8. Thermal ellipsoid diagram of $[(acac)_2RubptzRu(acac)_2]$.

and hydrophobic (Si/SiO_2/octadecyltrichlorosilane SAM, contact angle 105–110°) surfaces were soaked in an aqueous solution of the ion and then rinsed well with water. The surface binding properties of the +4 ions were assessed by X-ray photoelectron spectroscopy. N(1s) was observed in a 6.18 ± 0.92 ratio to Ru(3p) (theoretical value 6:1).

As shown in FIGURE 7, the atomic ratio of Ru(3p):Si(2p) reaches a constant value of 0.019 ± 0.002 after 0.5-h soaking time, indicating a self-limiting thin film has formed on the silicon dioxide. Unfortunately, the counterions also bind to the silicon dioxide surface. These stray charges are likely to be a problem for signal transmission in QCA.

Synthesis of $[(acac)_2RubptzRu(acac)_2]^{0,1+}$

In order to cut down on the charge of the molecule that would serve as a QCA cell, we designed a new mixed-valence Ru dimer in which the ammonia supporting ligands were replaced with acetylacetonate (acac) and the pyrazine bridge with 3,6-*bis*(2-pyridyl)-1,2,4,5-tetrazine (bptz).[17] Acac is an uninegative ligand that occupies two coordination sites on the ruthenium; bptz is neutral and also occupies two coordination sites, similar to 2,2′-bipyridine. Dark green $[(acac)_2Rubptz\ Ru(acac)_2]^0$ is obtained in 30% yield from refluxing $[(acac)_2Ru\ (CH_3CN)_2]$ with 0.5 eq bptz in acetone; the compound was analytically pure and was characterized by NMR, UV-Vis, mass spectroscopy, and single-crystal X-ray diffraction as the *meso* isomer shown in FIGURE 8.[15]

The compound showed two reversible oxidations (CH_2Cl_2, 0.1M $TBAPF_6$, Pt working and counterelectrodes, Ag/AgCl ref. electrode) at 0.17 V and 0.97 V due to successive oxidations of the two ruthenium(II) centers. The calculated compro-

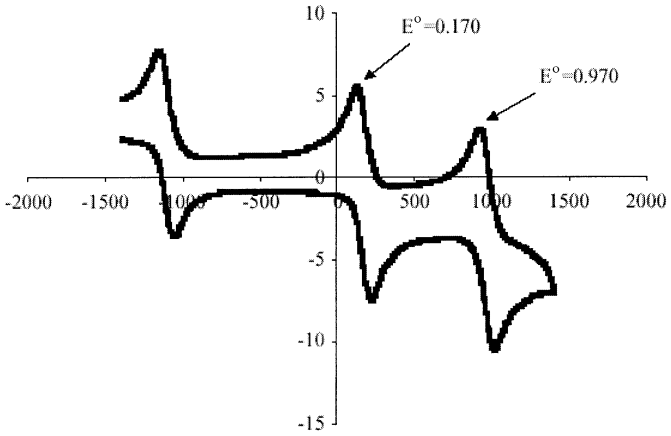

FIGURE 9. Cyclic voltammogram of $[(acac)_2RubptzRu(acac)_2]$, potential in mV vs. current in microamps; see text for experimental conditions.

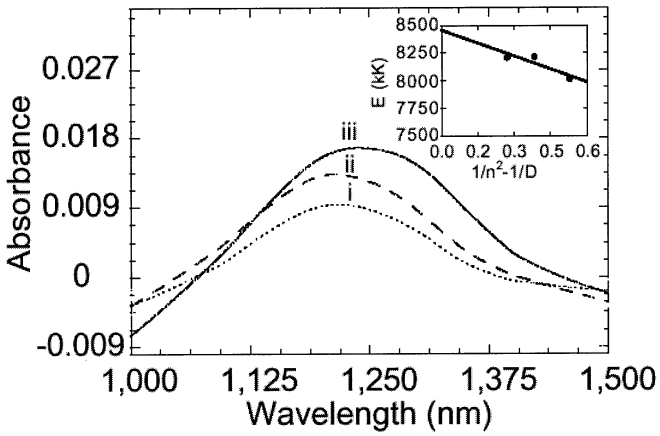

FIGURE 10. Near-IR spectroscopy of $[(acac)_2RubptzRu(acac)_2]^{1+}$ in (i) chloroform, (ii) acetonitrile, and (iii) methylene chloride; *inset* shows plot of band energy vs. solvent polarity function.

portionation constant is 10^{13}, comparable to the highest previously observed K_{com} values. Stoichiometric reaction with Ce(IV) gave the mixed-valence species $[(acac)_2RubptzRu(acac)_2]^{1+}$, isolated as its PF_6 salt, in quantitative yield (FIG. 9).

Charge Delocalization in $[(acac)_2RubptzRu(acac)_2]^{1+}$

This mixed-valence compound appears to be strongly delocalized, like the Creutz-Taube ion. A weak near-IR band (ε = 15–25) observed at 1220 nm was assigned as an intermetal charge transfer. In order to classify the mixed-valence ion as localized or delocalized, the peak position and peak width of this band was studied in solvents with different polarities (see FIG. 10).

The lack of dependence of the band on solvent polarity and its narrow width indicate that the charge is delocalized. QCA does not require that the ground state of each QCA cell be localized, only that the charge be capable of localization in the presence of an external perturbation. Therefore we have initiated studies on the surface attachment of this moderately charged mixed-valence species as a model QCA cell.

Formation of "Tracks" via Electron-Beam Lithography of Self-Assembled Monolayers (SAMs)

Surface attachment and organization of QCA cells is necessary for measurement of QCA cell and device properties. In the QCA paradigm, functional devices such as "wires," inverters, and majority logic gates are formed by placing tracks of identical QCA cells on a surface. If clocked arrays of cells (B. Toomarian and A. Fijany, personal communication, 2000) are used, the tracks can be up to ten QCA cells in width (10–30 nm wide). For molecular QCA, we envision an ultimate fabrication process that consists of selecting a molecule which packs properly in SAMs, laying down I/O structures lithographically, patterning a surface with "tracks" to which the QCA cells can bind, and dipping the patterned surface into a solution of the QCA cells to self-assemble the device.

We are using electron beam lithography (EBL) to fabricate tracks for molecular attachment and to make metal electrodes for interfacing with smaller detector structures. Our EBL system currently consists of a modified Amray 1400 scanning electron microscope (SEM) operating with a tungsten filament at 50 keV. We are currently modifying a Hitachi 30-keV cold cathode field emission SEM (CCFESEM) for lithography. The advantage of the CCFESEM is that the decreased thermal spread of electron energies in the beam results in lower chromatic aberrations and an attendant improvement in resolution; the width of the beam in the CCFESEM is about 1 nm compared to about 5 nm in the Amray. The main disadvantage to using CCFESEM systems is that the beam is inherently unstable, so variations in dose occur as a pattern is scanned. Dial *et al.* solved this problem with a similar instrument by using feedback from a spray aperture to control the dose in real time, and achieved excellent results in poly(methylmethacrylate) (PMMA) resist.[16] The ultimate goal is to achieve complex patterns with minimum features of less than 5 nm.

In order to make functional molecular QCA devices, the individual molecules must be attached to surfaces in ordered arrays. One approach to this problem is to make chemically distinct "tracks" in a self-assembled monolayer (SAM) of octadecyl trichlorosilane (OTS) on SiO_2. Electron-beam lithography offers one way to do this. The primary electron beam used to make the tracks shown in FIGURE 11 has a beam energy of about 50 keV. When this primary beam contacts the SAM, numerous secondary electrons of about 10 eV are produced, and these initiate chemical processes in the exposed portion of the SAM. The primary beam diameter is 5 nm, but due to dispersion of the secondary electrons, the smallest features we have been able to produce are larger. AFM characterization of the SAM after e-beam exposure (see FIG. 11) shows a track about 7 Å deep (the total height of the SAM is about 20 Å) and 30 nm in width.

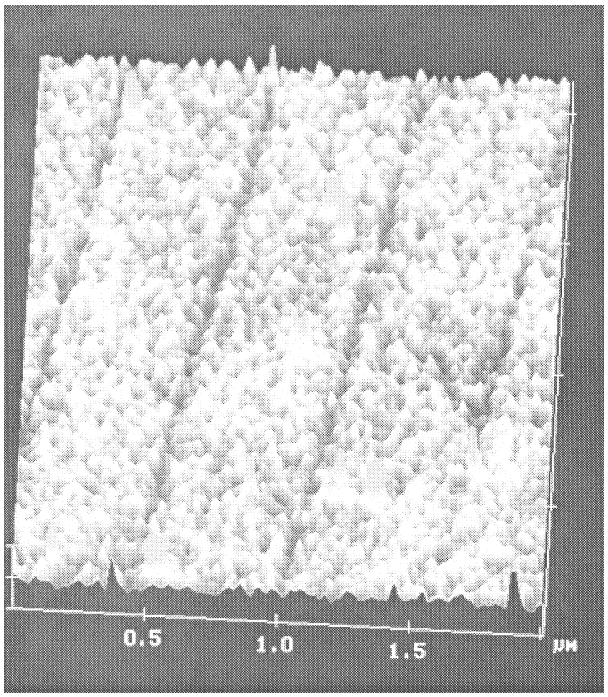

FIGURE 11. AFM image showing tracks fabricated in octadecyltrichlorosilane monolayer using electron-beam lithography.

The chemical nature of the bottom of these tracks cannot be directly determined. Large-area exposure of OTS SAMs to high energy electrons was carried out in the 8-MeV linear accelerator at the Notre Dame Radiation Laboratory. The beam diameter was over 1 cm. Before and after exposure to the beam, the SAMs were characterized by contact angle measurements and X-ray photoelectron spectroscopy. Exposed SAMs became significantly more hydrophilic (contact angle changed from ~110° to ~80°) and developed a large shoulder at high binding energy (BE 288–289 eV) in the C_{1s} region of the XPS. These changes, taken together with the 7-Å height decrease observed by AFM, are consistent with radical-initiated cleavage of the hydrocarbon chain to form functional groups such as alcohols, ketones, or carboxylic acids.

Surface Binding Properties of $[(acac)_2RubptzRu(acac)_2]^{0,1+}$

Three model surfaces (see FIG. 12) were used to probe the specificity of surface binding of $[(acac)_2RubptzRu(acac)_2]^{0,1+}$. In each case, a self-assembled monolayer with a different terminal functional group was formed and characterized, then exposed to a solution of ruthenium bptz dimer and recharacterized after thorough washing. The most hydrophilic surface was phosphonate-terminated; this surface gave advancing contact angles of <30°. A hydroxyl-terminated surface was used to model intermediate hydrophilicity; this surface gave contact angles of 35–52°. The

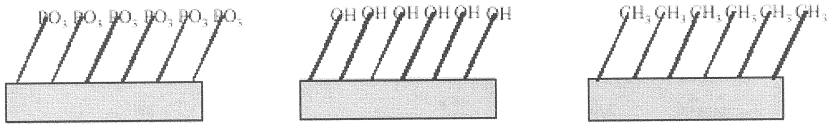

FIGURE 12. Three self-assembled monolayers of different surface hydrophobicity used in binding study.

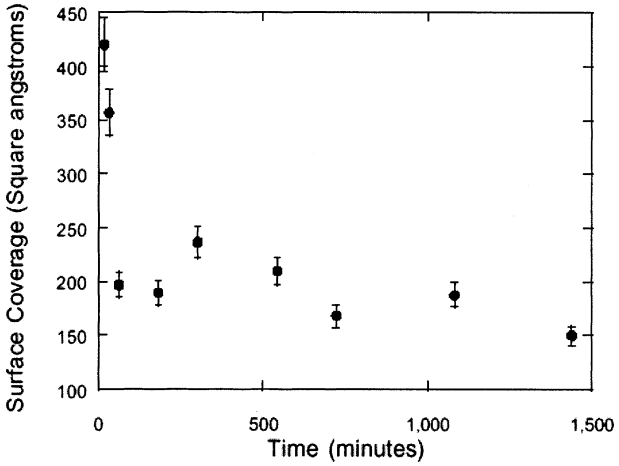

FIGURE 13. XPS study of binding of $[(acac)]_2RubptzRu(acac)_2]$ to phosphonate-terminated surface. Average surface area per molecule of $[(acac)_2RubptzRu(acac)_2]$ vs. soaking time.

most hydrophobic surface, terminated with methyl groups, gave contact angles of 105–110°.

Exposure of these surfaces to either $[(acac)_2RubptzRu(acac)_2]^0$ or $[(acac)_2RubptzRu(acac)_2]^{1+}$ gave similar results, as shown in FIGURE 13. Both metal species formed self-limiting monolayers on the phosphonate-terminated and hydroxyl-terminated surfaces, and neither bound detectably to the methyl-terminated surface. Monolayer formation was essentially complete after a 3-h soaking period. The atomic ratios of Ru, N, and bptz C are consistent with intact $[(acac)_2RubptzRu(acac)_2]$.

Long-chain thiols typically adopt a $\sqrt{3} \times \sqrt{3}$ R30° structure on gold(111) surfaces, which allocates ~22Å^2 to each thiol chain. By comparing the XPS peak areas from sulfur (or phosphorous) atoms with the peak areas due to ruthenium and nitrogen atoms, we were able to calculate the coverage of ruthenium dimers on these surfaces. The limiting coverage of $[(acac)_2RubptzRu(acac)_2]^{0,\,1+}$ was 170 ± 10 Å^2 per molecule, in reasonable agreement with the molecular dimensions.

Both oxidation states of the ruthenium dimer are persistently attached and cannot be rinsed off with solvent. Yet there is no specific anchoring group that attaches these molecules to the SAMs, as the thiol group anchors the individual molecules in the

underlying SAM to the gold. The similarity of binding specificity and coverage between the neutral $[(acac)_2RubptzRu(acac)_2]^0$ and the cationic $[(acac)_2RubptzRu(acac)_2]^{1+}$ suggests that the mechanism of binding is not electrostatic. For the cationic species, the counterion PF_6^- bound to the surface. The atomic ratio of F to Ru was 2.86± 0.3. This ratio would be 3.0 for $[(acac)_2RubptzRu(acac)_2]PF_6$. Since the PF_6 anion is retained, the cation is probably not binding to negative charges on the surface. Hydrogen bonding to the central tetrazine ring of the bptz ligand could be quite strong in the nonpolar solvents used for derivatization of the SAMs, and if such interactions operate in this inorganic monolayer, they represent a method for orienting as well as attaching individual molecules on the surface.

CONCLUSIONS

The QCA approach offers a natural match between device functionality and the intrinisic characteristics of molecules. Exploiting molecules as structured charge containers to encode binary information may provide a path to achieving truly single-molecule devices that have an architectural future. QCA devices have been demonstrated at larger length scales. Success at creating QCA devices at the molecular scale requires overcoming several challenges, not least that of measuring individual molecular charge states so that information can move up to the macroscopic world.

REFERENCES

1. HEATH, J.R. 2000. Wires, switches, and wiring. A route towards a chemically assembled nanocomputer. Pure Appl. Chem. **72:** 11–20; ELLENBOGEN, J.C. & J.C. LOVE. 2000. Architectures for molecular electronic computers: 1. Logic structures and an adder designed from molecular electronic diodes. Proc. IEEE **8:** 386–426; METZGER, R.M. 2000. Unimolecular rectification down to 105K and spectroscopy of hexadecylquinolinium tricyanoquiodimethanide. Syn. Met. **109:** 23–28; REED, M.A. 1999. Molecular-scale electronics. Proc. IEEE **87:** 652–658; SCHUMM, J.S., D.L. PEARSON, L. JONES & J.M. TOUR. 1996. Potential molecular wires and alligator clips. Nanotechnology **7:** 430–433.
2. CHEN, J., M.A. REED, A.M. RAWLETT & J.M. TOUR. 1999. Large on-off ratios and NDR in a molecular electronic device. Science **286:** 1550–1552.
3. TOUR, J.M, M. KOZAKI & J.M. SEMINARIO. 1998. Molecular scale electronics: a synthetic/computational approach to digital computing. J. Am. Chem. Soc. **120:** 8486–8493.
4. LENT, C.S. 2000. Molecular electronics: bypassing the transistor paradigm. Science **288:** 1597–1599; LENT, C.S., P.D. TOUGAW, W. POROD & G.H. BERNSTEIN. 1993. Quantum cellular automata. Nanotechnology **4:** 49–57; SNIDER, G.L. *et al*. 1999. J. APPL. PHYS. **85:** 4283–4285; POROD, W. *et al*. 1999. Quantum-dot cellular automata: computing with coupled quantum dots. Int. J. Electron. **86:** 549–590.
5. TOUGAW, P. D., C.S. LENT & W. POROD. 1993. Bistable saturation in coupled quantum-dot cells. J. Appl. Phys. **74:** 3558; TOUGAW, C.S. & C.S. LENT. 1994. Logical devices implemented using quantum cellular automata. J. Appl. Phys. **75:** 1818–1825.
6. TOUR, J.M. 1996. Conjugated macromolecules of precise length and constitution. Organic synthesis for the construction of nanoarchitectures. Chem. Rev. **96:** 537–553.
7. LENT, C.S. & P.D. TOUGAW. 1997. Device architecture for computing with quantum dots. Proc. IEEE **85:** 541–557.

8. ORLOV, A.O. *et al.* 1997. Realization of a functional cell for quantum-dot cellular automata. Science **277:** 928–930; AMLANI *et al.* 1999. Digital logic gate using quantum-dot cellular automata. Science **284:** 289–291; see also Ref. 13.
9. FULTON, T.A. & G.H. DOLAN. 1987. Observation of single-electron effects in small tunnel junctions. Phys. Rev. Lett. **59:** 109–112.
10. SAMUELSON, L. & G.S. SNIDER. 2000. Unpublished results.
11. C.S. LENT, P.D. TOUGAW & W. POROD. 1994. Quantum cellular automata: the physics of computing with arrays of quantum dot molecules. Proc. Workshop on Physics and Computing: 5–13. IEEE Computer Society Press. New York.
12. ANANTRAM, M.P. & V. ROWCHOWDHURY. 1996. Can metastable states affect ground-state computing? Proc. 4th Workshop on Physics and Computation: 17–21. New England Complex Systems Institute.
13. AMLANI, I. *et al*. 1998. Demonstration of six-dot quantum cellular automata system. Appl. Phys. Lett. **72:** 2179–2181.
14. CREUTZ, C. & H. TAUBE. 1973. J. Am. Chem. Soc. **95:** 1087.
15. CHELLAMMA, S. & M. LIEBERMAN. 2001. Synthesis and properties of $[Ru_2(acac)_4(bptz)^{n+}$ (n=0,1) and crystal structure of $[RU_2(acac)_4(bptz)]$. Inorg. Chem. **40:** 3177–3180.
16. DIAL, O., C.C. CHENG & A. SCHERER. 1998. Fabrication of high-density nanostructures by electron beam lithography. J.Vac. Sci.Technol. B **16**(6): 3887–3890.
17. CHELLAMMA, S. & M. LIEBERMAN. 2001. Synthesis and properties of $[Ru_2(acac)_4(bptz)]^{n+}$ (n = 0,1) and crystal structure of $[Ru_2(acac)_4(bptz)]$. Inorg. Chem. **40:** 3177–3180.